

# RCS Reduction of Patch Array Using Shorted Stubs Metamaterial Absorber

Dhawan Singh and Viranjay M. Srivastava

Department of Electronic Engineering, Howard College, University of KwaZulu-Natal, Durban - 4041, South Africa

Email: dhawan\_deor@ieee.org; viranjay@ieee.org

**Abstract** –A novel design approach for the out of band radar cross section (*RCS*) reduction of a conventional  $2 \times 2$  patch antenna arrays using shorted stubs metamaterial absorber (*MMA*) operating in X-band has been proposed. Firstly, an ultrathin *MMA* unit cell with a central frequency of 10 GHz is designed and its scattering parameters, absorbance characteristics and polarization sensitivity have been analyzed. Then, a patch antenna array has been designed at a resonant frequency of 7.54 GHz. Simulation and experimental results exhibit that when patch antenna array is loaded with *MMA*, its monostatic and bistatic *RCS* response reduces significantly for the horizontal as well for vertical polarization. However, it has negligible influence on the radiation characteristics, whilst the bandwidth, gain and overall performance of patch array preserved simultaneously. Finally, a compatibility of observation achieved between simulated and measured results.

**Index Terms**—Antenna array, Frequency selective surfaces (*FSS*), Metamaterial absorber (*MMA*), Patch antenna, Radar cross section (*RCS*).

## I. INTRODUCTION

Metamaterials have attained tremendous attention and possess several different and unique properties that make it suitable for wide range of applications in microwave regime [1], [2]. In immediate past, there has been growing a sense of concern in utilizing *MMA* structure in the electromagnetic (*EM*) and antenna engineering to enhance the stealth capabilities. Radar cross section (*RCS*) reduction plays an important role in stealth and military based applications.

The *RCS* of an object means how much it is detectable and visible to radar. So if the *RCS* of an object is more it is more visible to radar. So, it is of prime importance to reduce the detection, visibility and thus enhance the stealth capability of the target device by the enemy radar. It has been found that antenna is the important contributor to the total *RCS* and one should reduce the *RCS* of the antennas.

The formal proficiency of radar absorption for instance shaping and Radar Absorbing Material (*RAM*) technique cannot be enforced, as it might reduce the antenna performance [3], [4]. Several other *RCS* reduction

techniques have been employed and available in the literature for the patch antenna. Jang et al used electronic band gap (*EBG*) structure to reduce the *RCS* of patch antenna array using a conducting polymer [5]. Shiv Narayan et al designed a less detectable antenna using active hybrid-element frequency selective surface (*FSS*) structure for avoiding detection [6]. Zheng et al designed a wideband microstrip antenna using artificial magnetic conductor (*AMC*) structures to improve the stealth capability of the antenna [7].

Compared to above three structures, this novel *MMA* structure is likewise one of the prospective solution and a new research focus that offers excellent features as ultrathin, near-unity absorbance, highly polarization insensitive to oblique angle of incidence [8]-[13]. Thus, make it more compatible with antennas designs for the reduction of *RCS* in stealth technology whereas preserving the antenna radiation performance [14]-[18].

Owing to its advantages, patch antennas are used to a great extent today because of its simple design, linearly polarized, conformability to planar and non-planar structures, cost-effective, ease of implementation and compatible with the circuit board technology. Therefore, a lot of research is focusing on *RCS* reduction of single patch antenna structure [19]-[21]. But this type of antenna having some disadvantages and suffers from low radiation performance such as its narrow bandwidth, directivity, lower gain, and radiation efficiency.

So it cannot be used for long-distance communication especially in military applications, where a radar system is used to scan the electromagnetic beam quickly throughout the sky to detect the planes and missiles and contrariwise. Numerous techniques have been advised to improve its radiation preformation. One of the vital solutions is a combination of the patch antenna so-called antenna array. It has been found that when several antenna elements are combined to form an array, its overall radiation performance enhances furthermore [22]-[24].

One of the problems with previous *MMA* designs is *RCS* reduction achieved at the cost of the increased size of the substrate. Thus, this does not support miniaturization and turn out to be the unreliable and uneconomical solution [25]-[27]. Therefore, we have tried to achieve the *RCS* reduction without increasing the periodicity of antenna unit cell structure. Again, it has been found that when the gap between multiple antennas

---

Manuscript received February 16, 2018; revised November 23, 2018.  
Corresponding author email: dhawan\_deor@ieee.org.  
doi:10.12720/jcm.13.12.702-711

reduces, their performance starts degrading and that influence factors like gain and radiation efficiency because of the mutual coupling among them. By using MMA capability of suppressing surface waves propagation in a given frequency range, one can compensate for these losses [28].

In this research work, we have proposed and designed a  $2 \times 2$  rectangular patch antenna array using shorted stubs metamaterial absorber (MMA) for the reduction of RCS at operating frequency resonant at 10 GHz. The prototype structure is simulated, fabricated and tested. The simulation result shows a reduction of -10 dBsm for *x-polarization* (*x-p*) and -9.93 dBsm for *y-polarization* (*y-p*) incidence wave at 10 GHz resonant frequency obtained. This is incongruous with the measured data and provides adequate ground for the proposed structure in improving the stealth capabilities of the antenna array.

The remaining paper has been outlined as follows: Section II explains characteristics of the shorted stubs MMA structure and shows that absorbing mechanism and polarization-insensitivity to the oblique angle of incidence have been achieved. The performances of an

antenna array with loading MMA structure are analyzed in connection with the referenced patch antenna array in Section III. Then *monostatic* and *bistatic* radar cross section of the conventional antenna array and MMA loaded antenna array has been analyzed in Section IV. Finally, the work has been concluded and the future directions are recommended in Section V.

## II. METAMATERIAL ABSORBER DESIGN ASPECTS

Today, with the growing demand and stringent interest for various applications such as low detectable objects for stealth technology, the attention is to design near unity MMA structure with ultrathin and polarization insensitive characteristics. As shown in Fig. 1, a MMA based on shorted stubs and split rectangular bars have been designed and fabricated. Fig. 1(a) gives a glimpse of designing process and shows how transformation is made from the simple circular ring to shorted stubs and split rectangular bars to get a passive tuned MMA absorber that operates at X-band.

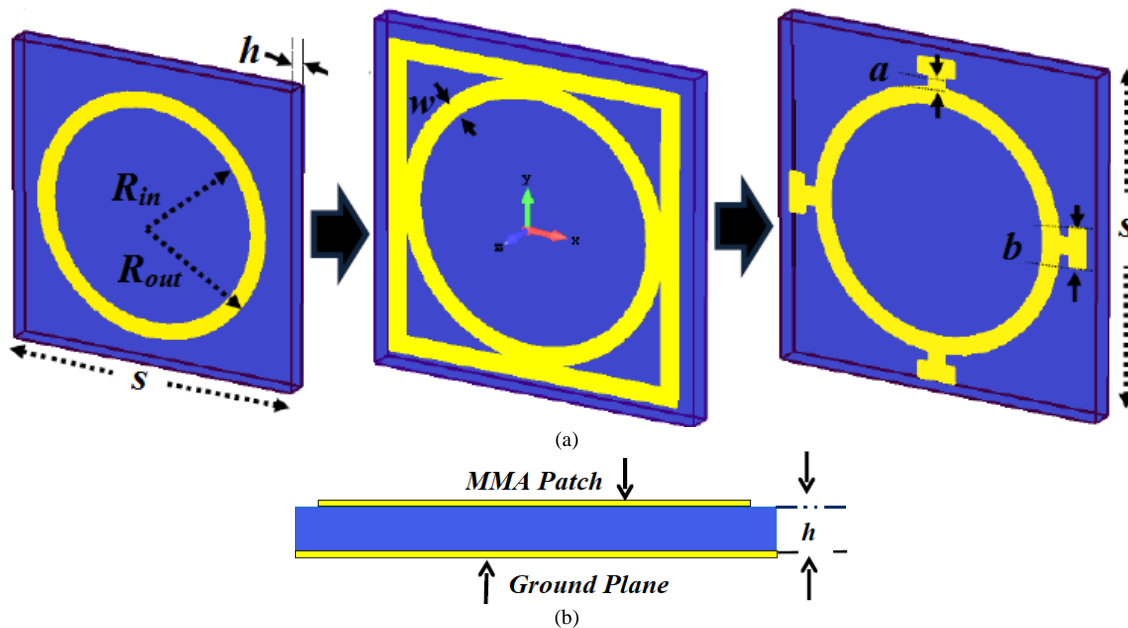


Fig. 1. A Metamaterial Absorber with shorted stubs and split rectangular bars (a) Front view and (b) side view. Unit cell dimensions:  $S = 5$  mm,  $R_{in} = 1.5$  mm,  $R_{out} = 1.75$  mm,  $a = w = 0.25$  mm,  $h = 0.40$  mm and  $t = 0.035$  mm

It has been found that by varying the dimensions of shorted stubs ( $a$ ) and rectangular bar length ( $b$ ), we can adjust the resonant frequency to entire X-band to Ku-band [13]. Here MMA is tuned to the central resonant frequency of 10 GHz by mean of varying length of shorted stubs and split square rectangular bars. The periodicity ( $S$ ) and the thicknesses ( $h$ ) for the shorted stubs MMA is designed to 5 mm and 0.4 mm respectively.

The side view of MMA unit cell has been shown in Fig. 1(b). All the parameters of MMA are optimized and adjusted to obtain a sharp frequency resonance peak at 10 GHz. A resonance curve has been plotted between absorbance  $A(\omega)$ , reflectance  $R(\omega)$  and transmittance  $T(\omega)$

as shown in Fig. 2(a). An absorbance of 99.95 % achieves and that approximates to unity absorbance.

A graph for reflection coefficient  $S_{11}$  has been plotted between simulated and measured results in Fig. 2(b). This indicates that the measured results are in good agreement with simulated ones with a marginal reduction in reflection coefficient parameters from -40.41 dB to -22.67 dB. A simulation analysis has been also made for oblique angle of incidence ( $\theta$ ) and polarization sensitivity ( $\phi$ ) for TE modes of Electromagnetic (EM) waves as depicted in Fig. 2(c) and 2(d) respectively.

This MMA operates at wide operating angles where absorbance remained above 94% for  $\theta$  varies between  $0^\circ$

and  $50^\circ$  and after it starts reducing. For  $\theta$  equals to  $70^\circ$  it becomes equal to 72.58%. However, it remains highly polarisation sensitive with the variation of  $\phi$ . Since this

structure possesses symmetry property so  $TM$  mode analysis of  $EM$  wave has not considered for this research work.

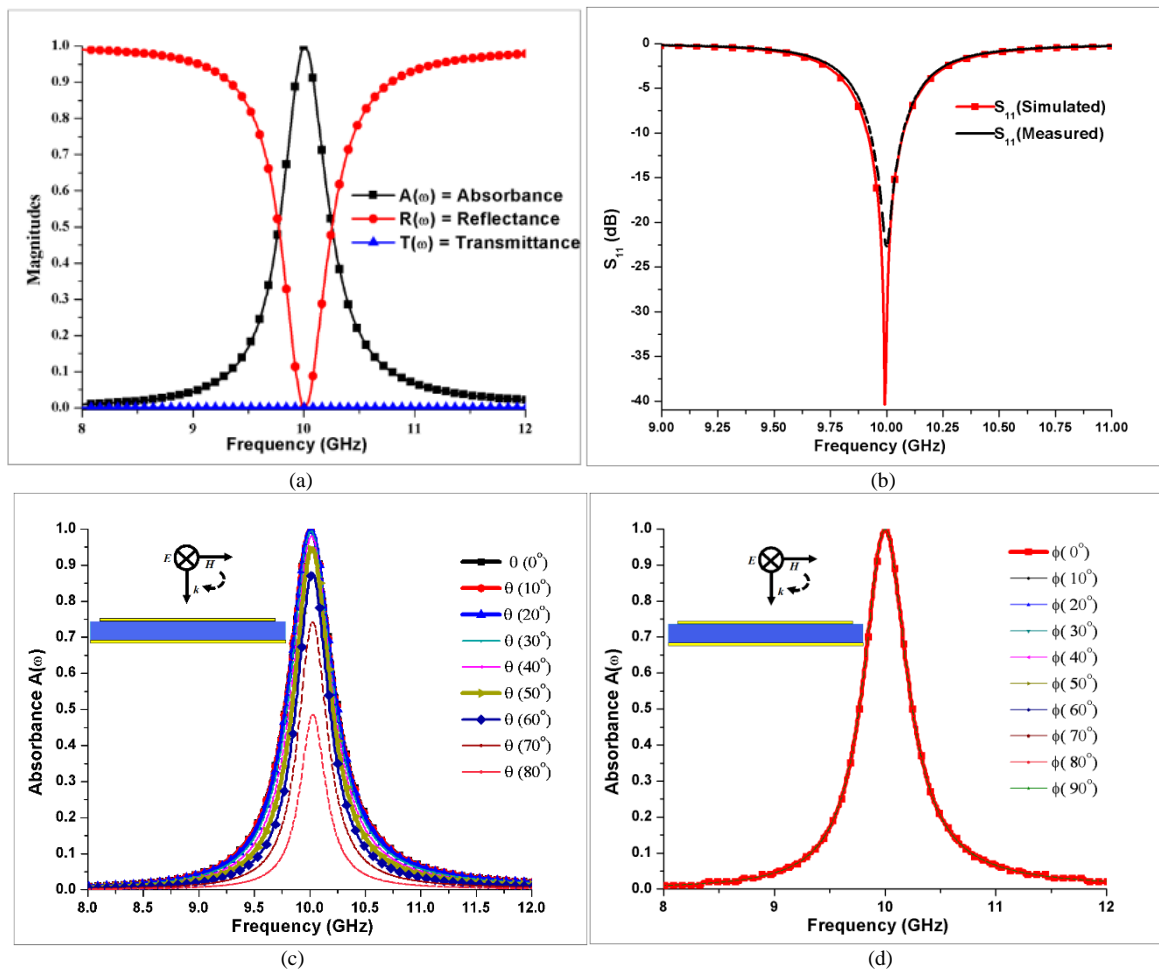


Fig. 2. Resonance Curves for (a)  $A(\omega)$ ,  $R(\omega)$  and  $T(\omega)$ , (b) Comparison between simulated and measured  $S_{11}$  response (c) Oblique Angle of Incidence ( $\theta$ ) and (d) Polarization Sensitivity ( $\phi$ ) for TE modes of MMA.

### III. LINEAR ARRAY ANTENNA DESIGN ASPECTS

For long distance communication, single element antenna is insufficient to fulfill the gain or radiation pattern requirement. So making an array could be a possible solution. The antenna array is a process of placing many antennas all together with an exact number of elements, amplitude, spacing, and phasing based on the target application.

Proper spacing and phasing are required so that the individual radiation will meet at the point of interest in a constructive way and in other direction they will cancel out each other because of destructive interference. So that we will get a very high directional pattern with higher directivity and gain in the desired direction without getting anything in the other direction that offers applications in radar and terrestrial communication. But practically it doesn't cancel out in other directions leads to side lobes.

Phase distribution to the individual element decides how the fields that are meeting at the point of interest and modifies the side lobe level and the main lobe direction.

The surface area or aperture of the complete radiating structure is decided on the basis of a total number of elements and their spacing. A larger aperture size enhances its gain performance and a larger spacing enhances its directivity. For this research work, we have restricted our study to  $2 \times 2$  antenna elements.

A  $\lambda/2$  element spacing value has been chosen to avoid side lobes occurrence [29]. Although it increases directivity when the element spacing approaches to  $\lambda$ . Multiple unwanted grating lobes appear when element spacing value goes beyond  $\lambda$  so become impractical. Here, we have considered element spacing ( $g$ ) of  $\lambda/2$  that approximates to 20 mm with respect to the central frequency of 7.5GHz as shown in Fig. 3(a). In this research work, the antenna elements are fed with the same amplitude, equal phase and uniform spacing results in a planar antenna array.

The basic structure of the proposed patch antenna array is depicted in Fig. 3. It is designed to operate at 7.53 GHz resonant frequency by varying and optimizing its physical parameters. The top layer is the radiating patch made up of copper-backed by a most popular, low cost and readily

available flame retardant FR4 substrate with  $\tan \delta$  is 0.025 and  $\epsilon_r$  is 4.3. The substrate is grounded using a copper layer. The periodicity ( $L_s$ ) of Patch Antenna array

is 50 mm  $\times$  50 mm with the length of the radiating Patch ( $l$ ) is 9.17 mm. The length of the central substrate is 10 mm whereas the central substrate height ( $h_1$ ) is 1 mm.

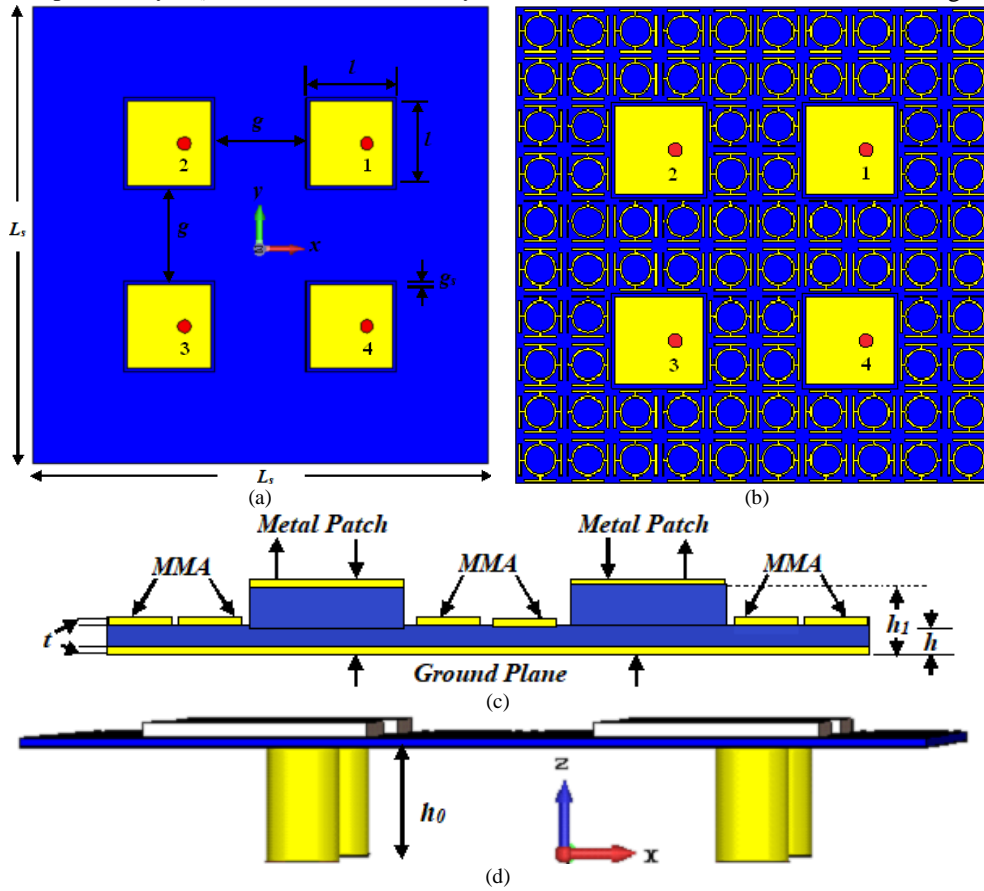


Fig. 3. A coaxial feed patch antenna (a) Proposed antenna array, (b) MMA loaded patch antenna array, (c) Side view of proposed Antenna and (d) side view with coaxial feed.

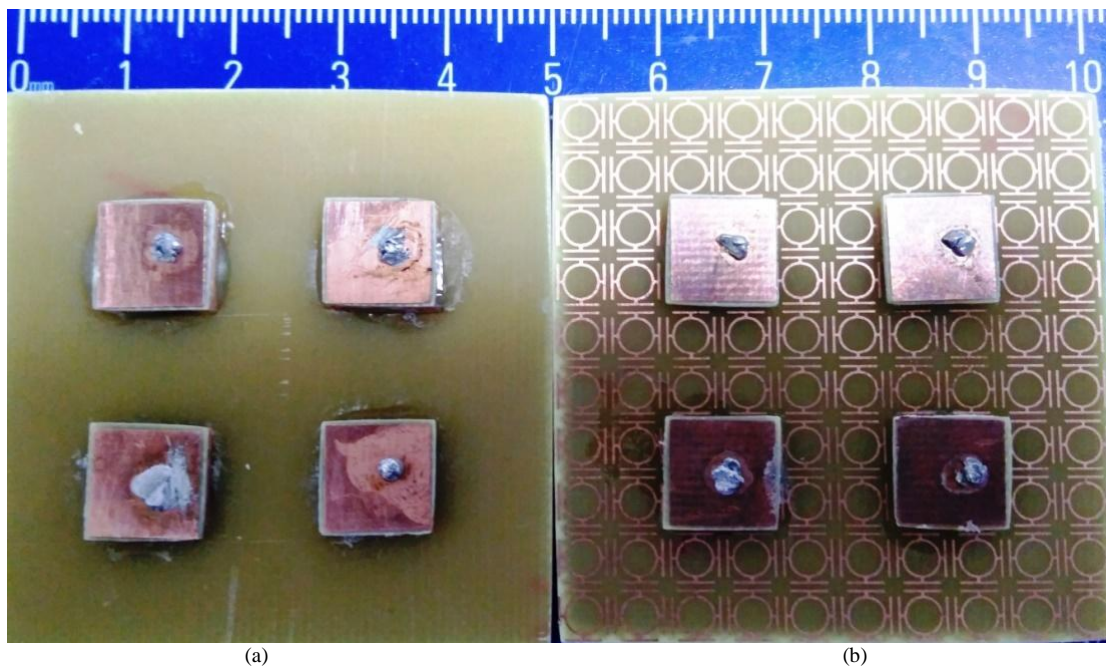


Fig. 4. Fabricated antenna array (a) Referenced antenna array and (b) Proposed antenna array structure

The thickness of the remaining surrounded area ( $h$ ) is 0.4 mm where MMA is designed. All the parameters

description has been given in Table I. The design of a conventional patch antenna array has been shown in Fig.

3(a) with its parameters. While Fig. 3(b) shows the modified MMA loaded patch antenna array. A side view of the modified structure is depicted in Fig. 3(c).

The fabricated reference and proposed antenna array view have been given in Fig. 4(a) and 4(b), respectively. The feeding technique used for the antenna is very important when we consider the RCS reduction of the antenna because it controls the antenna scattering characteristics.

TABLE I: ANTENNA PARAMETER DESCRIPTION

Description	Dimensions (mm)	Parameters
$L_s$	50	Periodicity of Structure
$h_1$	1	height of substrate
$l$	9.17	Length of Patch
$g$	10	Element Spacing
$g_s$	0.83	Gap b/w Patch and MMA
$t$	0.035	Thickness of metal
Pos_x	1.68	Position of Probe
$h_0$	5	Height of connector

An antenna suffers from two types of scattering namely Structural Mode and Antenna Mode Scattering. If the antenna is fed by properly matched loads, there will be only structural mode scattering. But when the antenna is not fed by perfectly matched loads there will be both scatterings that mean a part of the energy will be reflected and reradiate back to space.

A coaxial feed technique provides the low RCS since its feeding network is on the other side of the dielectric material as compared to the microstrip feeding technique. So MMA absorber based technique is most suitable for the reduction of RCS. As we cannot change the antenna structure parameters since it influences the frequency response behavior.

However, it has been found that when the Patch antenna surrounded by MMA structure, it immensely reduces the RCS effect on the system without compromising with the performance of the antenna. Thus, one can minimize the structural mode RCS as low as possible and hence emerged as a new design technique.

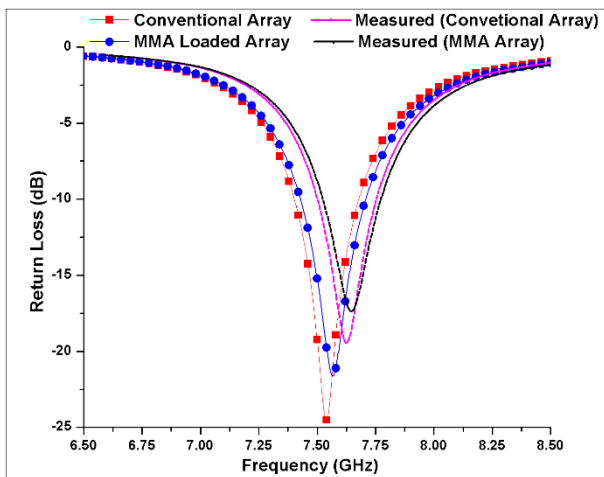


Fig. 5. A comparison of return loss ( $S_{11}$ ) curve for patch antenna array.

Each patch element has been fed by coaxial feed with its central position approximates to  $50 \Omega$  matching the impedance at the position,  $pos\_x = 1.68$  mm and  $pos\_y = 0$  as shown in Fig. 3(d). Its frequency response is optimized at 7.54 GHz. Then, the antenna structure is modified and loaded with  $10 \times 10$  MMA unit cell. A total of  $2 \times 2$  MMA unit cells are etched out for the antenna array. To minimize the mutual coupling and keep the antenna radiation performance unaffected a small gap ( $g_s$ ) of 0.83 mm is kept between MMA and each Patch element. A comparison of scattering parameters ( $S_{11}$ ) has been made between the conventional antenna array and modified antenna array with the measured results and is shown in Fig. 5.

The  $S_{11}$  for a conventional antenna array occurs at 7.54 GHz with resonance peak magnitude of -24.52 dB. When it is loaded with MMA unit cells then the return loss ( $S_{11}$ ) for a modified antenna array occurs at 7.57 GHz with resonance peak magnitude of -21.64 dB. The measured results for both structures has been also shown that indicates that for the conventional antenna the resonance peak for  $S_{11}$  is obtained at 7.53 GHz with the magnitude of -19.45 dB while for MMA loaded antenna array the value for  $S_{11}$  occurred at 7.55 GHz with the magnitude of -17.37 dB.

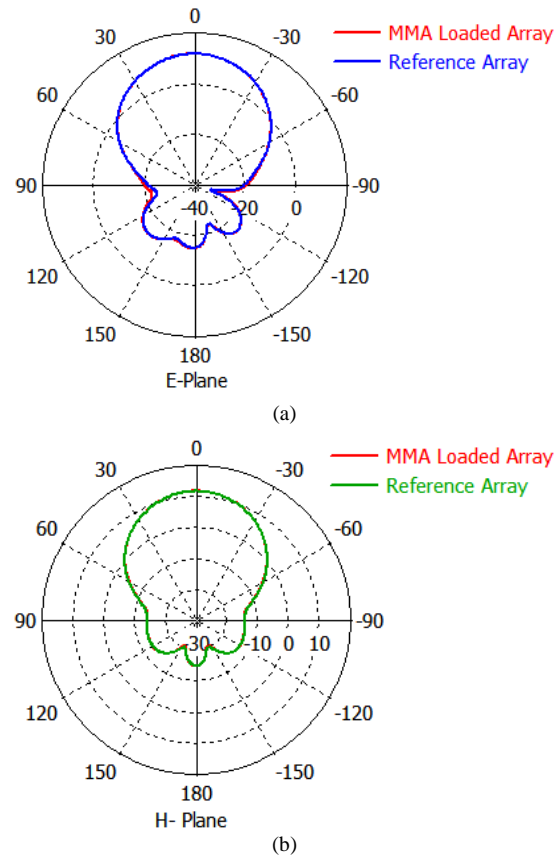


Fig. 6. An analysis of simulated radiation pattern between reference patch array antenna and MMA loaded patch Antenna for (a)  $\phi = 0^\circ$  and (b)  $\phi = 90^\circ$ .

The value for -10 dB bandwidth for conventional antenna array came out to be 274 MHz that is 3.63 % of

resonant frequency however for modified antenna array it came out to be 278 MHz that is 3.67 % of resonant frequency. So a small increment in bandwidth is observed with a modified MMA loaded antenna array. An analysis of radiation pattern between the referenced antenna and MMA loaded patch antenna has been made and is shown in Fig. 6.

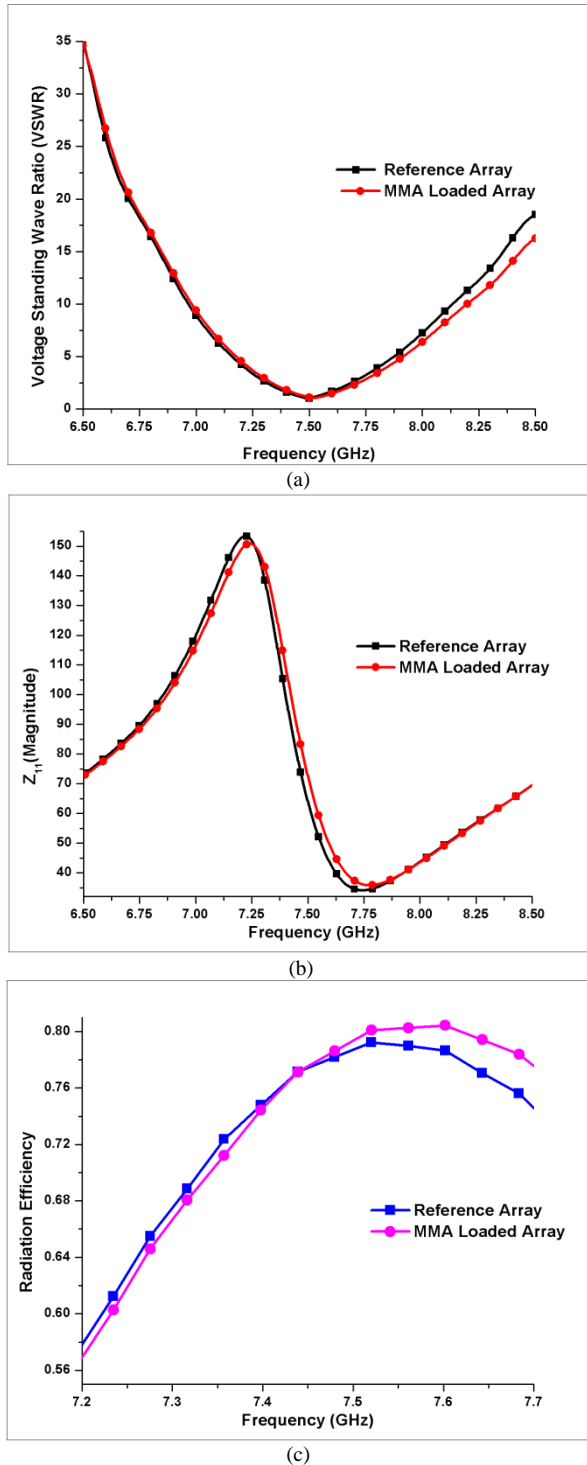


Fig. 7. Comparison of simulated results (a) VSWR (b)  $Z_{11}$  (c)  $\eta$  between the referenced array and proposed MMA loaded Patch array.

For *E-Plane*, the reference patch array operating frequency resonant peak occurs at 7.54 GHz with main

lobe magnitude is 11.6 dBi with the direction is at  $0^\circ$  and 3 dB angular width  $49^\circ$  while sidelobe level is -25.4 dB. For MMA loaded Patch array the is at  $0^\circ$  and 3 dB angular width  $48.7^\circ$  while sidelobe level is -25.4 dB as shown in Fig. 6(a).

For *H-Plane*, the operating frequency resonant the peak occurs at 7.57 GHz with main lobe magnitude is 11.7 dBi with the direction reference patch array operating frequency resonant peak occurs at 7.54 GHz with main lobe magnitude is 11.6 dBi with the direction is at  $0^\circ$  and 3 dB angular width  $50.5^\circ$  while sidelobe level is -25.3 dB. For MMA loaded Patch array the operating frequency resonant peak occurs at 7.57 GHz with main lobe magnitude is 11.7 dBi with the direction is at  $0^\circ$  and 3 dB angular width  $50.2^\circ$  while sidelobe level is -25.4 dB as shown in Fig. 6(b).

A comparison of voltage standing wave ratio (VSWR), impedance ( $Z_{11}$ ) and radiation efficiency ( $\eta$ ) has been made between the conventional antenna array and MMA loaded antenna array as depicted in Fig. 7. The simulated value of VSWR for reference patch array operating at 7.54 GHz resonance frequency is 1.27, whilst for MMA loaded Patch array operating at 7.57 GHz resonance frequency is 1.30, which is within the acceptable range from 1.0 to 2.0 as depicted in Fig. 7(a).

The simulated value of  $Z_{11}$  for reference patch array operating at 7.54 GHz resonance frequency is 52.59  $\Omega$ , whilst for MMA loaded Patch array operating at 7.57 GHz resonance frequency is 52.89  $\Omega$ , which is approximately matched to 50  $\Omega$  resistance as depicted in Fig. 7(b). Similarly, a simulation analysis is made to find out the efficiency of antenna and it has been found that for reference patch array operating at 7.54 GHz the radiation efficiency comes out to be 79.48 %, whereas for MMA loaded Patch array operating at 7.57 GHz a slight rise in radiation efficiency is found and equal to 80.26 % as shown in Fig. 7(c).

TABLE II: COMPARISON OF ANTENNA PERFORMANCE

Structure/Performance Parameters	Referenced Antenna	Modified Antenna
Frequency (f)	7.54 GHz	7.57 GHz
Return Loss ( $S_{11}$ )	-24.52	-21.64
Bandwidth (-10 dB)	274 MHz (3.63 %)	278 MHz (3.67 %)
Directivity	11.6 dBi	11.7 dBi
Gain Value	9.22 dB	9.39 dB
Radiation Efficiency ( $\eta$ )	79.48	80.26
VSWR	1.27	1.30
Impedance ( $Z_{11}$ )	52.59	52.89

Thus the MMA loaded antenna not only enhances the stealth capabilities of antenna array but antenna radiation performance including gain, directivity, bandwidth, and radiation efficiency are found to increase marginally. A complete comparison between all the antenna performances has been given in Table II that signify the

relevance and importance of this proposed antenna array design.

#### IV. RADAR CROSS SECTION REDUCTION OF MMA LOADED ANTENNA ARRAY

As compared to conventional antenna geometry, *monostatic RCS* of the *MMA* loaded patch antenna array is almost polarization independent. *Monostatic RCS* of the conventional array and *MMA* loaded array for *x-p* and *y-p* incidence wave have been shown in Fig. 8(a) and 8(b) respectively with its measured values. A table has been also drawn for the purpose of comparison and is depicted in Table III. From the figure, it has been found that the value for *monostatic RCS* reduced throughout observation band after loading it with *MMA* unit cells. However at 10 GHz resonant frequency, the significant peak reduction in *monostatic RCS* for *MMA* loaded antenna array is -20.41 dBsm for *x-p* and -20.25 dBsm for *y-p* incidence wave.

TABLE III: COMPARISON OF MONOSTATIC RCS

Structure / Frequency (GHz)	Referenced Antenna(dBsm)		Modified Antenna(dBsm)	
	x-p	y-p	x-p	y-p
6	-15.47	-15.33	-15.46	-15.35
6.5	-15.28	-15.04	-15.35	-15.14
7	-15.49	-15.25	-15.67	-15.23
7.5	-18.24	-22.62	-18.80	-25.22
8	-13.50	-12.40	-13.88	-12.52
8.5	-11.78	-11.37	-11.97	-11.47
9	-11.12	-10.93	-11.42	-11.16
9.5	-10.73	-10.60	-11.43	-11.28
10	-10.40	-10.32	-20.41	-20.25
10.5	-10.05	-10.02	-10.51	-10.46
11	-9.74	-9.70	-9.82	-9.79
11.5	-9.39	-9.37	-9.44	-9.44
12	-8.95	-8.95	-9.03	-9.03

A total reduction for *monostatic RCS* is up to 10 dBsm for *x-p* and 9.93 dBsm for *y-p* incidence wave as compared with the referenced antenna. For conventional antenna array, the measured *monostatic RCS* peaks are observed at -10.41 dBsm for *x-p* and -10.24 dBsm for *y-p*. Although for *MMA* loaded antenna, the measured *monostatic RCS* peaks are observed at -16.12 dBsm for *x-p* and -16.32 dBsm for *y-p*.

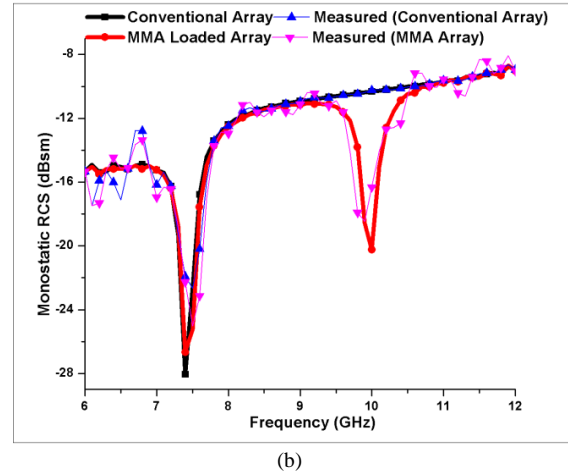
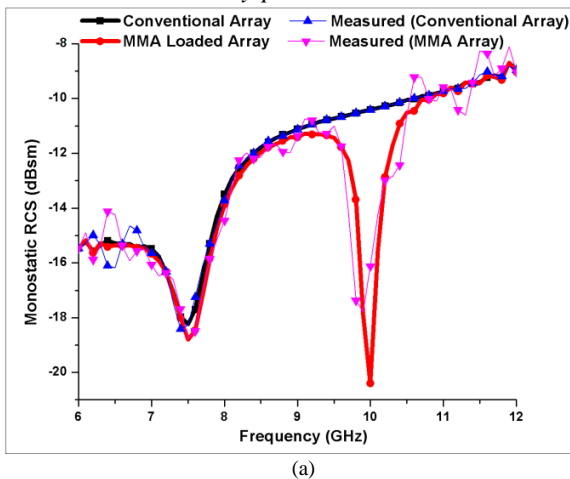


Fig. 8. Comparison of Monostatic RCS for normal Incidence (a) *x-p* polarized incidence wave (b) *y-p* polarized incidence wave

Minor deviations in simulated and measured results are recorded because of fabrication, handling, and testing of structure that can be ignored. Hence, the measured *RCS* values for antenna array are in good agreements with the simulation results. A simulation analysis of conventional array antenna and *MMA* loaded array antenna has been also made for *bistatic RCS* and depicted in Fig. 9.

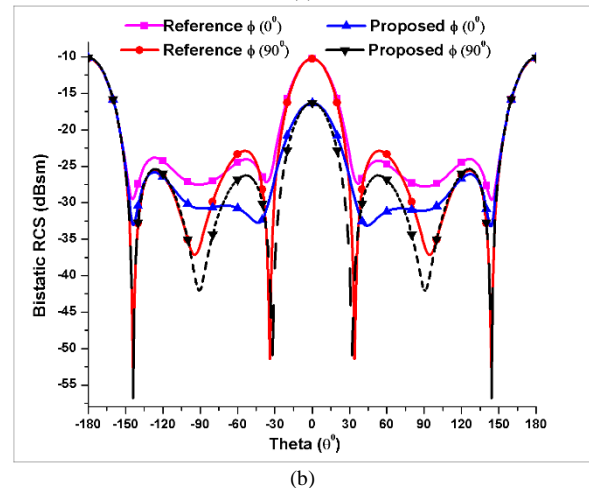
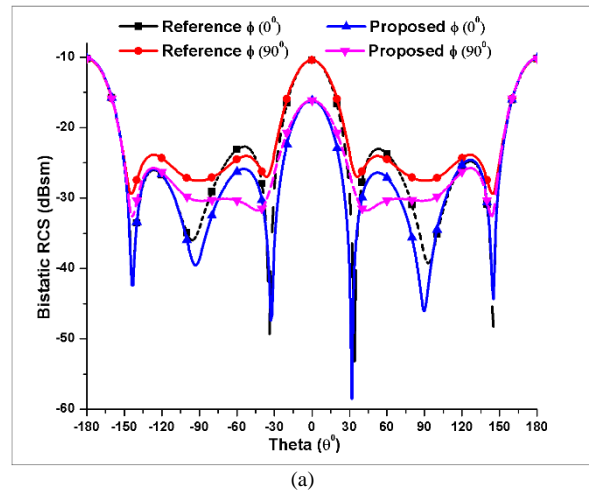


Fig. 9. Comparison of bistatic RCS between the referenced array and proposed *MMA* Antenna array for (a) horizontal polarization (b) vertical polarization at 10 GHz.

For horizontal polarization at  $\varphi = 0^\circ$ , the *bistatic RCS* of the referenced antenna array and proposed antenna array have been simulated and analyzed at 10 GHz. The *bistatic RCS* of the *MMA* loaded antenna array reduced throughout the angle  $\theta$  with a significant reduction in between  $-110^\circ$  to  $96^\circ$ . The maximum reduction between the referenced antenna array and *MMA* loaded antenna array observed of 11.75 dBsm at  $-32^\circ$  and 22.08 dBsm at  $32^\circ$  respectively as shown in Fig. 9(a).

At  $\varphi = 90^\circ$ , the *bistatic RCS* of the *MMA* loaded antenna array reduced significantly for angle  $\theta$  in between  $-154^\circ$  to  $154^\circ$ . The maximum reduction between the referenced antenna array and *MMA* loaded antenna array observed of 7.13 dBsm at  $-48^\circ$  and 7.13 dBsm at  $48^\circ$  respectively as shown in Fig. 9(a).

For vertical polarization at  $\varphi = 0^\circ$ , the *bistatic RCS* of the referenced antenna array and proposed antenna array have been simulated and analyzed at 10 GHz. The *bistatic RCS* of the *MMA* loaded antenna array reduced throughout the angle  $\theta$  with a significant reduction in between  $-157^\circ$  to  $157^\circ$ .

The maximum reduction between the referenced antenna array and *MMA* loaded antenna array observed of 7.94 dBsm at  $-48^\circ$  and 8.23 dBsm at  $48^\circ$  respectively as shown in Fig. 9(b). At  $\varphi = 90^\circ$ , the *bistatic RCS* of the *MMA* loaded antenna array reduced significantly for angle  $\theta$  in between  $-33^\circ$  to  $33^\circ$ . The maximum reduction between the referenced antenna array and *MMA* loaded antenna array observed of 16.51 dBsm at  $-32^\circ$  and 16.51 dBsm at  $32^\circ$  respectively as shown in Fig. 9(b).

## V. CONCLUSION AND FUTURE SCOPE

In this research work, we have proposed a shorted stubs metamaterial absorber operating at 10 GHz of the resonant frequency in *X-band*. A comparison has been made between reference antenna array and *MMA* modified antenna array. It has been found that when *MMA*s are loaded in a rectangular  $2 \times 2$  patch antenna arrays, it significantly reduces the *RCS* of the structure throughout the observation band. Henceforth increase the stealth capability of the structure.

However, maximum resonance peak reduction is observed in 10 GHz at which *MMA* has been designed. The *monostatic* and *bistatic RCS* analysis have been made for *x-p* as well as for *y-p* of incidence wave. The overall radiation performance of antenna array with and without *MMA* remains preserved and unaffected. Even though, the gain, directivity, bandwidth and radiation efficiency found marginally increased. Because of the limitation on size and some very common errors during the fabrication process, then measurement precision, a slight variation in measured results observed with respect to simulated one.

This structure finds its applications in stealth technology for military planes, space aircraft, missiles, ships, and other sensitive vehicles for long distance wireless communication.

## REFERENCES

- [1] D. Singh and V. M. Srivastava, "3-D Cylindrical shaped frequency selective surface," in *Proc. IEEE 4th International Conference on Advanced Computing and Communication Systems (ICACCS-2017)*, Coimbatore, India, January 6-7, 2017, pp. 1-6.
- [2] D. Singh and V. M. Srivastava, "Polarization insensitive cylindrical shaped frequency selective surface," in *Proc. IEEE 10th International Conference on Development in eSystem Engineering (DeSe2017)*, Paris, France June, 14-16, 2017, pp. 1-6.
- [3] L. Zhou and F. Yang, "Radar cross section reduction for microstrip antenna using shaping technique," in *Proc. IEEE International Conference on Microwave and Millimeter Wave Technology (ICMMT)*, Beijing, China, June 5-8, 2016, pp. 871-873.
- [4] G. G. Peixoto, A. L. de Paula, L. A. Andrade, C. M. A. Lopes, and M. C. Rezende, "Radar absorbing material (RAM) and shaping on radar cross section reduction of dihedral comers," in *Proc. SBMO/IEEE MTT-S International Conference on Microwave and Optoelectronics*, Brasilia, Brazil, 25-25 July 2005, pp. 460-463.
- [5] H. K. Jang, J. H. Shin, and C. G. Kim, "Low RCS patch array antenna with electromagnetic bandgap using a conducting polymer," in *Proc. IEEE International Conference on Electromagnetics in Advanced Applications*, Sydney, Australia, September 20-24, 2010, pp. 140-143.
- [6] S. Narayan, B. Sangeetha, T. V. Sruthi, V. Shambulingappa, and R. U. Nair, "Design of low observable antenna using active hybrid-element FSS structure for stealth applications," *AEU-International Journal of Electronics and Communications*, vol. 80, pp. 137-143, October 2017.
- [7] Y. Zheng, J. Gao, X. Cao, Z. Yuan, and H. Yang, "Wideband RCS reduction of a microstrip antenna using artificial magnetic conductor structures," *IEEE Antennas and Wireless Propagation Letters*, vol. 14, pp. 1582-1585, August 2015.
- [8] D. Singh and V. M. Srivastava, "Dual resonances shorted stub circular rings metamaterial absorber," *AEU-Journal of Electronics and Communication*, vol. 83, pp. 58-66, January 2018.
- [9] A. Bhattacharya, S. Bhattacharyya, S. Ghosh, D. Chaurasiya, and K. V. Srivastava, "An ultrathin penta-band polarization-insensitive compact metamaterial absorber for airborne radar applications," *Microwave and Optical Technology Letters*, vol. 57, no. 11, pp. 2519-2524, November 2015.
- [10] M. Pu and X. Ma, "Design of a patch antenna with dual-band radar cross section reduction," in *Proc. International Conference on Microwave and Millimeter Wave Technology*, Shenzhen, China, May 5-8, 2012, pp. 1-3.
- [11] D. Singh and V. M. Srivastava, "Triple band regular decagon shaped metamaterial absorber for X-band applications," in *Proc. IEEE International Conference on Computer Communication and Informatics*, Coimbatore, India, January 5-7, 2017, pp. 411-415.

- [12] K. Ozden, O. M. Yucedag, and H. Kocer, "Metamaterial based broadband RF absorber at X-band," *AEU - International Journal of Electronics and Communications*, vol. 70, no. 8, pp. 1062-1070, August 2016.
- [13] D. Singh and V. M. Srivastava, "Metamaterial absorber based on concentric rings with shorted stubs," in *Proc. IEEE International Conference on Engineering and Technology (ICET-2016)*, Coimbatore, India, December 16-17, 2016, pp. 159-163.
- [14] S. K. Patel, C. Argyropoulos, and Y. P. Kosta, "Broadband compact microstrip patch antenna design loaded by multiple split ring resonator superstrate and substrate," *Waves in Random and Complex Media*, vol. 27, no. 1, pp. 92-102, June 2016.
- [15] J. Baviskar, A. Mulla, A. Baviskar, D. Auti, and R. Waghmare, "Performance enhancement of microstrip patch antenna array with incorporation of metamaterial lens," in *Proc. IEEE Aerospace Conference*, Yellowstone, USA, March 5-12, 2016, pp. 1-10.
- [16] Y. Li, K. Zhang, L. A. Yang, and L. Du, "Gain enhancement and wideband RCS reduction of a microstrip antenna using triple-band planar electromagnetic band-gap structure," *Progress in Electromagnetics Research Letters*, vol. 65, pp. 103-108, January 2017.
- [17] Y. Zhao, J. Gao, X. Cao, T. Liu, L. Xu, X. Liu, and L. Cong, "In-band RCS reduction of waveguide slot array using metasurface bars," *IEEE Transactions on Antennas and Propagation*, vol. 65, no. 2, pp. 943-947, February 2017.
- [18] D. Singh and V. M. Srivastava, "An analysis of RCS for dual-band slotted patch antenna with a thin dielectric using shorted stubs metamaterial absorber," *AEU-Journal of Electronics and Communication*, vol. 90, pp. 53-62, June 2018.
- [19] A. Shater and D. Zarifi, "Radar cross section reduction of microstrip antenna using dual-band metamaterial absorber," *Applied Computational Electromagnetics Society Journal (ACES)*, vol. 32, no.2, pp. 135-140, February 2017.
- [20] Z. X. Zhang and J.C. Zhang. "RCS reduction for patch antenna based on metamaterial absorber," *Progress in Electromagnetic Research Symposium (PIERS)*, Shanghai, China, August 8-11, 2016, pp. 364-368.
- [21] T. Liu, X. Cao, J. Gao, Q. Zheng, W. Li, and H. Yang, "RCS reduction of waveguide slot antenna with metamaterial absorber," *IEEE Transactions on Antennas and Propagation*, vol. 61, no. 3, pp. 1479-1484, March 2013.
- [22] M. Z. Joozdani, M. K. Amirhosseini and A. Abdolali, "Wideband radar cross-section reduction of patch array antenna with miniaturized hexagonal loop frequency selective surface," *Electronics Letters*, vol. 52, no. 9, pp. 767-768, April 2016.
- [23] J. Zheng, S. Fang, Y. Jia, and Y. Liu, "RCS reduction of patch array antenna by complementary split-ring resonators structure," *Progress in Electromagnetics Research C*, vol. 51, pp. 95-101, June 2014.
- [24] J. Zhang, J. Wang, M. Chen, and Z. Zhang, "RCS reduction of patch array antenna by electromagnetic band-gap structure" *IEEE Antennas and Wireless Propagation Letters*, vol. 11, pp. 1048-1051, August 2012.
- [25] X. Liu, J. Gao, X. Cao, Y. Zhao, W. Li, S. Li, and N. Li, "A high-gain and low-scattering waveguide slot antenna of artificial magnetic conductor octagonal ring arrangement," *Radio Engineering*, vol. 25, no. 1, pp. 46-52, April 2016.
- [26] W. Li, S. Yang, J. Zhang, S. Sai, H. Yuan, and S. Qu, "The RCS reduction of microstrip antenna design based on multi-band metamaterial absorber," in *Proc. IEEE MTT-S International Microwave Workshop Series on Advanced Materials and Processes for RF and THz Applications (IMWS-AMP)*, Suzhou, China, July 1-3, 2015, pp. 1-3.
- [27] J. Mu, H. Wang, H. Wang, and Y. Huang, "Low-RCS and gain enhancement design of a novel partially reflecting and absorbing surface antenna," *IEEE Antennas and Wireless Propagation Letters*, vol. 16, pp. 1903-1906, March 2017.
- [28] X. J. Gao, T. Cai, and L. Zhu, "Enhancement of gain and directivity for microstrip antenna using negative permeability metamaterial," *AEU-Journal of Electronics and Communication*, vol.70, no.7, pp. 880-885, 2016.
- [29] I. V. Minin and O. V. Minin, "The brief elementary basics of antenna arrays," *Springer*, Berlin, Heidelberg, 2008, vol. 19, pp. 1-70.



**Er. Dhawan Singh** received his M.Sc. Degree in Electronics from the Jiwaji University, Gwalior, M.P, India in 2006. He also received M. Tech. degree in Electronics and Communication from Eternal University, Baru Sahib, Sirmour, H.P, India in 2013. He qualified UGC-NET in December 2014 in Electronics

Science. He worked as Asst. Prof. in the Department of Electronics and Communications, Akal College of Engineering and Technology, Eternal University, Baru Sahib, India. He has more than 10 years of experience in teaching, industry, and research. He is currently working towards a Ph.D. from the School of Electrical, Electronic and Computer Engineering, University of KwaZulu-Natal, Durban, South Africa. His research interest includes Antenna design, Metamaterial Absorbers, Embedded systems, and Wireless communications.



**Prof. Viranjay M. Srivastava** is a Doctorate (2012) in the field of RF Microelectronics and VLSI Design, Master (2008) in VLSI design, and Bachelor (2002) in Electronics and Instrumentation Engineering. He has worked for the fabrication of devices and development of circuit design. Presently,

he is a faculty in Department of Electronic Engineering, Howard College, University of KwaZulu-Natal, Durban, South Africa. He has more than 13 years of teaching and research experience in the area of VLSI design, RFIC design, and Analog IC design. He has supervised various Bachelors, Masters and Doctorate theses. He is a senior member of IEEE, and member of IEEE-HKN, IITPSA, ACEEE, and IACSIT. He has worked as a reviewer for several Journals and Conferences

both national and international. He is author/co-author of more than 110 scientific contributions including articles in international refereed Journals and Conferences and also author of following books, 1) VLSI Technology, 2) Characterization of

C-V curves and Analysis, Using VEE Pro Software: After Fabrication of MOS Device, and 3) MOSFET Technologies for Double-Pole Four Throw Radio Frequency Switch, Springer International Publishing, Switzerland, October 2013.